ARCHIVES OF TRANSPORT *ISSN (print):* *0866-9546*
Volume 64, Issue 4, 2022 ***e-ISSN (online):*** *2300-8830*
DOI: *10.5604/01.3001.0016.1051*

MODELLING THE ACOUSTIC SIGNATURE AND NOISE PROPAGATION OF HIGH SPEED RAILWAY VEHICLE

Krzysztof POLAK[1], Jarosław KORZEB[2]

[1] *Railway Track and Operation Department, Railway Institute, Warsaw, Poland*

[2] *Faculty of Transport, Warsaw University of Technology, Warsaw, Poland*

Abstract:

The proportion of high speed railway vehicles in the rolling stock of national carriers providing public transport services is constantly increasing. Currently, Alstom vehicles run at the highest speed on railway lines in Poland. The paper attempts to identify the acoustic signature of high speed railway vehicles. There are many works and studies aimed at identifying or defining the acoustic signature of high speed railway vehicles. However, the authors of these works carried out their research in a rather narrow scope, i.e. the measurement cross-section had only 1 or 2 measurement points with one microphone at each point. As part of the conducted experimental research, the location of testing grounds was determined, the measurement apparatus was selected and the methodology for carrying out measurements including the assessment of noise emission on curve and straight line were specified for electric multiple units. The object of the tests were railway vehicles of Alstom company, type ETR610, series ED250, the so-called Pendolino, moving on a selected measuring route without stops at a speed of 200 km/h. Measurements were carried out on the railway line no. 4 Grodzisk Mazowiecki – Zawiercie, section Grodzisk Mazowiecki - Idzikowice at kilometre 18+600 (curve) and 21+300 (straight section). When measuring the acoustic signals with a microphone array (4x2), 8 measurement microphones operating in the audible range were used. The microphones were placed at a distance of 5 m, 10 m, 20 m and 40 m from the track centre, at a height of 4 m (from the rail head) and at the rail head (approx. 0.8 m from the ground surface). In addition, an acoustic camera with 112 directional microphones was used to locate the main noise sources, which was located at a distance of approximately 20 m from the track centreline. The identification of the main noise sources for high speed railway vehicles, basig on actual acoustic measurements, made it possible to isolate the dominant noise sources, as well as to find out the amplitude-frequency characteristics in the range from 20 Hz to 20 kHz, divided into one third octave bands.

Keywords: *noise emissions, railway noise, increased speed railways, environmental noise impact*

To cite this article:

Polak, K., Korzeb, J., (2022). Modelling the acoustic signature and noise propagation of high speed railway vehicle. Archives of Transport, 64(4), 73-87. DOI: https://doi.org/10.5604/01.3001.0016.1051

Contact:
1) kpolak@ikolej.pl [https://orcid.org/0000-0002-1464-7214] – corresponding author; 2) jaroslaw.korzeb@pw.edu.pl [https://orcid.org/0000-0002-1889-4925]

1. Introduction

The proportion of higher-speed railway vehicles in the rolling stock of operators providing public transport services is constantly increasing. Currently, Alstom's vehicles of type ETR610, series ED250 (the so-called Pendolino) are allowed to run on railway lines at the highest speed in Poland. These vehicles can travel at a maximum speed of 250 km/h, however, due to technical limitations of the railway infrastructure, their maximum operating speed on the Central Railway Line (railway line no. 4 Grodzisk Mazowiecki - Zawiercie) is equal to 200 km/h. (Żurkowski, 2015)

An analysis of the literature has shown that there are many works and studies aimed at identifying or determining the acoustic signature of railway vehicles. However, the authors of these works carried out research within a rather narrow scope, i.e. the measurement cross-section had only 1 or 2 measurement points with one microphone at each point. Most measuring points were located at a distance of 7.5 m from the track axis at a height of 1.2 m from the rail head and/or at a distance of 25 m at a height of 3.5 m, counting from the rail head (Graf et al., 2019) or (He et al., 2014) or (Jiang et al., 2018) or (Li L. et al., 2019) or (Maillard et al., 2020) or (Němec et al., 2020) or (Zea et al., 2017) or (Zhang et al., 2018) or (Zhao et al., 2018). The cited studies mainly involved high speed vehicles travelling at speeds above 200 km/h (Lan at al., 2021) or (Sheng et al., 2020) or (Zhang et al., 2019) or (Zhang et al., 2018). In addition, a review of available publications and studies carried out to date in Poland reveals a lack of available studies on the characteristics of the dominant noise sources generated by the analysed high speed railway vehicles.

Experimental tests were carried out to enable the development of an acoustic signature for the analyzed vehicle by measuring acoustic phenomena using an acoustic camera and a 4x2 microphone array. The distribution of measurement points at distances of 5 m, 10 m, 20 m and 40 m from the track axis, with 2 microphones located both at the level of the head of the rail and at 4 m above the level of the head of the rail, made it possible to parameterize the spatial distribution of the phenomenon of sound wave propagation in the close vicinity as a function of travel time, distance and frequency. The measurements carried out made it possible to identify the dominant noise sources in case of high speed railway vehicles travelling at 200 km/h and to understand the spectral characteristics of these sources.

The experimental studies carried out and the database built as part of the work, containing the actual waveforms in the time and frequency domain, served as a source of information on the generated impacts for the sake of modelling noise propagation in close surroundings. Selected models of the assessment of railway noise propagation were analysed. On the basis of the conducted experimental studies, the behaviour of selected models describing the change in the sound level in the i-th frequency band as a function of variable distance of the observer from the railway line on which high speed railway vehicles are operated was verified. In addition, the author's model is presented, together with a database built as part of the work, containing actual waveforms in the time and frequency domain.

2. Technical specification of test objects

The object of the experimental research was Alstom's railway vehicles type ETR610, series ED250 series – Pendolino (Fig. 1). These vehicles are managed by the largest operator in Poland - PKP Intercity S.A. They are two-way electric multiple units consisting of seven sections, including four motor sections (two end sections on both sides) and three trailer sections (Raczyński, 2018) or (Wawrzyniak, 2013).

Fig. 1. Research object –Alstom ETR610 type, ED250 series vehicle – Pendolino (source: own elaboration)

The standard-gauge vehicles (suitable for 1435 mm gauge track operations) are equipped with 8 traction motors, asynchronous, three-phase, with a power of

708 kW each. The length of the vehicle is equal to 187.4 m and its weight is equal to 395.5 tonnes. The train is suitable for passenger service at stations with a platform height of 760 mm and 550 mm above the rail head, as well as at lower platforms up to a height of 250 mm with use of a special step (Graff, 2016).
The bodies of the ETR 610 series vehicles are made of lightweight aluminium alloy profiles, while the bogie frame is of steel construction. The trains have propulsion systems with motors built entirely under the carriage bodies, from which power is transmitted to the wheelset via an articulated Cardan shaft and axial bevel gear. The vehicles use two-axle bogies with one driving axle and one rolling axle, with very low masses and fitted with torsion dampers to ensure the vehicle has adequate dynamic characteristics on curves at speeds of 250 km/h.(Czarnecki et al., 2018) or (Wawrzyniak, 2013).
The vehicle was equipped with two braking systems: an air brake (steel discs and sintered pads) and an electromagnetic rail brake. The average acceleration of the vehicle on a horizontal straight section is 0,36 m/s2. (Wawrzyniak, 2013).
Two sections (a straight section and a curve) of the railway track located on railway line No. 4 Grodzisk Mazowiecki - Zawiercie (Central Railway Main Line - CMK), section Grodzisk Mazowiecki - Idzikowice, were selected for experimental research. A detailed description of the location of the gauge section is presented in Chapter 3.
According to the Polish Railway Lines Instruction (2009), railway line no. 4 Grodzisk Mazowiecki - Zawiercie, is a trunk line, electrified, with mostly double-track and a maximum design speed of 250 km/h.
The area in the vicinity of the survey cross-sections is constituted mainly of agricultural and rural areas, with single family houses (the nearest buildings located behind the survey cross-section at a distance of approximately 15-20 m).
A detailed description of the survey objects has been presented in previous publications, including (Polak et al., 2022) or (Polak et al., 2021) or (Polak et al., 2019).

3. Methodology of the conducted experimental studies

Acoustic signal measurements were carried out in 2019 in the summer period (August) on railway line No. 4 Grodzisk Mazowiecki - Zawiercie, section Grodzisk Mazowiecki - Idzikowice, in two locations:

- curve – approx. 18+600 km (m. Świnice, Długa street),
- straight section – approx. 21+300 km (m. Szeligi, Dojazdowa street).

The measurements were made on working days (Monday-Friday), 2 days each, at each of the two measurement cross-sections between 08:00 and 20:00.
The area around the track bed, at both locations where acoustic signals were measured, is mainly agricultural land and rural areas. In the case of the measurement cross-section location at km 18+600 (curve), the area consists mainly of agricultural land (opposite side of the track bed with respect to the measurement cross-section). A farmstead with single-family houses is located a short distance (20 m) behind the measurement cross-section. The area around the cross-section at km 21+300 (straight section) is mainly agricultural. On the opposite side of the measurement cross-section, at a distance of approx. 35 m, there are forest areas.
The measurements were conducted under weather conditions without precipitation. The average air temperature ranged from 20.4 oC to 24.6 oC, average humidity: from 48.9% to 58%, average atmospheric pressure ranged from 997 hPa to 1008.5 hPa, and the average wind speed did not exceed 4.4 m/s.
The recording of acoustic events from high-speed railway vehicles was carried out using measurement equipment consisting of the following devices:

- Noise Inspector Bionic M-112 acoustic camera,
- two Svantek sound level meters - SVAN 979,
- a four-channel sound level meter from Svantek - SVAN 958A,
- two Svantek sound level meters - SVAN 955,
- measuring microphones (electro-acoustic transducers) from Svantek - 8 pcs,
- Svantek acoustic calibrator SV 36 Class 1,
- speed meter
- Davis Instruments Vantage Pro2 weather station.

The test objects were Alstom railway vehicles of ETR610 type, ED250 series, travelling along a selected measuring route without stopping at a speed of 200 km/h. Measurements were taken on a straight section and a curve (R=4000 m).
During the noise measurements with the microphone array (4x2), 8 measurement microphones operating

in the audible band were used. The microphones were placed at a height of 4 m (from the rail head) and at the rail head (approx. 0.8 m from the ground surface). In addition, an acoustic camera located approximately 20 m from the track axis was used to locate the main noise sources. A schematic of the measurement cross-section during the experimental tests carried out is shown in Fig. 2. The results obtained were subjected to acquisition using Svantek's dedicated software, SvsnPC ++, which enabled to generate data for further analysis and processing, in line with the assumptions. Noise measurement with the microphone array was carried out using a continuous method, i.e. all acoustic phenomena were measured during the experimental tests. The recording of individual passages (type of vehicle, time of day) made it possible in the subsequent work to select only the ones pertaining to the test object.

4. Development of an acoustic signature for a high speed railway vehicle

Recognition of the acoustic signature of high speed vehicles operating in Polish conditions was possible by identifying the main noise sources generated by the test object using an acoustic camera and obtaining a time history, recorded for each passage of the test vehicle separately (with a step of 1 s), containing the average sound level LAeq for each second of the passage and obtaining the noise frequency spectrum for each second, divided into one-third octave bands within the audible band, i.e. from 20 Hz to 20 kHz.

4.1. Identification of the main noise sources

The Noise Inspector Bionic M-112 acoustic camera, equipped with 112 directional microphones, was used to determine the main noise sources. Thanks to the mounted optical camera, the image is assigned to the distribution of sound pressure levels. The acoustic camera uses, among other things, the beamforming method for measurements, which allows results to be obtained in the frequency range from 400Hz to 24kHz, with a sampling rate of approximately 12Hz. The beamforming method involves processing a spatial-temporal signal recorded by a microphone array. Each microphone of the acoustic array, having a specific position relative to the centre of the array, is assigned with time delays, thanks to which it is possible to focus the signal beam in the direction of acoustic wave propagation (Abualhayja'a et al., 2021) or (Gade et al., 2015) or (Graf et al., 2019) or (Le Courtois et al., 2016) or (Zhang, Squicciarini et al., 2019).

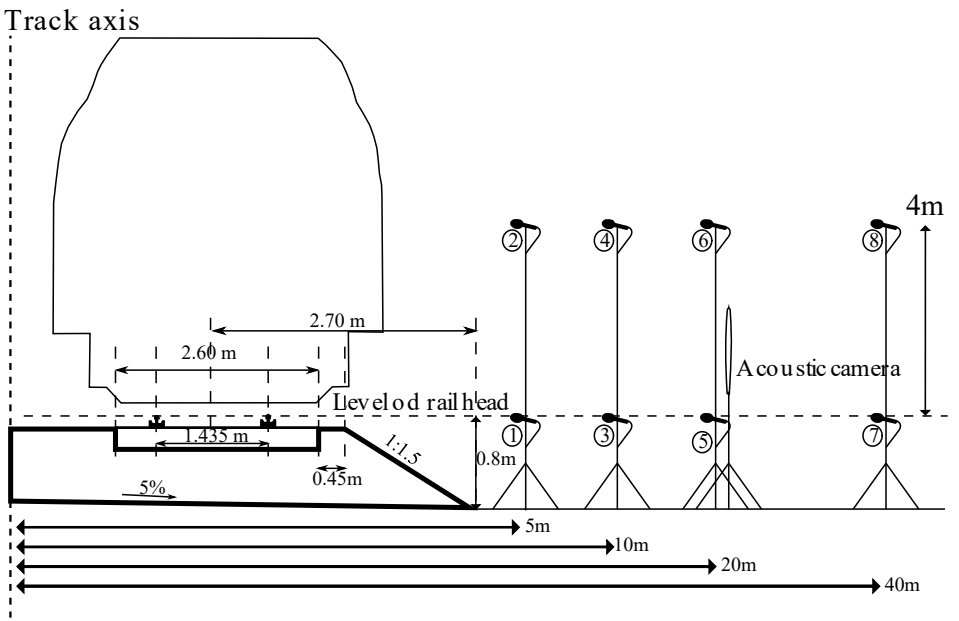

Fig. 2. Instrumented cross-section during experimental testing (source: own elaboration)

By using a time delay, the measured signal is the same for all microphones used. The signal received by the microphones, delayed by an appropriate time, is summed at the output of the array and thus amplified compared to a measurement that uses only one microphone (Chiariotti et al., 2019) or (Li M. et al., 2021) or (Meng et al., 2015) or (Uda et al., 2018). On the basis of the target measurements carried out in August 2019, the main source of noise generated by higher-speed railway vehicles travelling at around 200km/h was defined. In order to better illustrate the results obtained, the acoustic events characterised by the highest noise levels were grouped into three frequency ranges, i.e. 500-1000 Hz, 1000-2000 Hz and 2000-3000 Hz (Fig. 3 and Fig. 4).

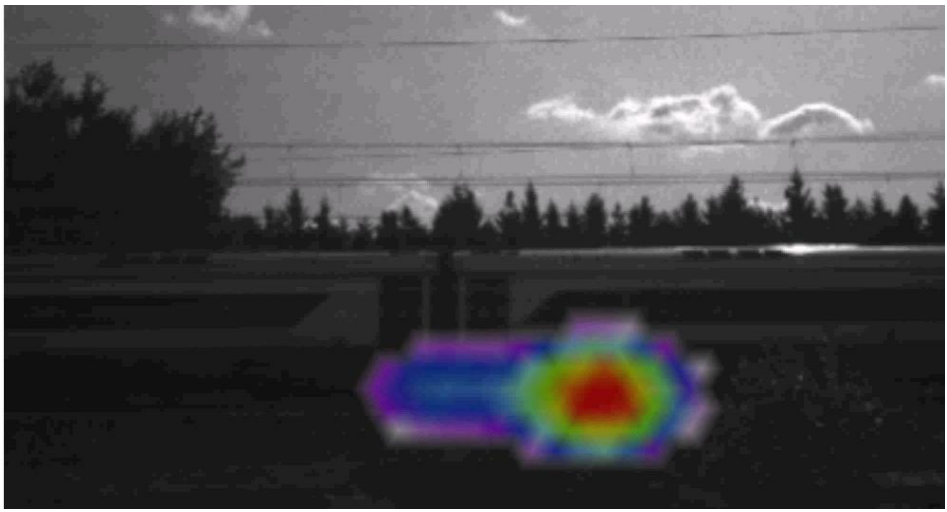

Fig. 3. Sound level distribution in the frequency range 500-1000 Hz - straight section

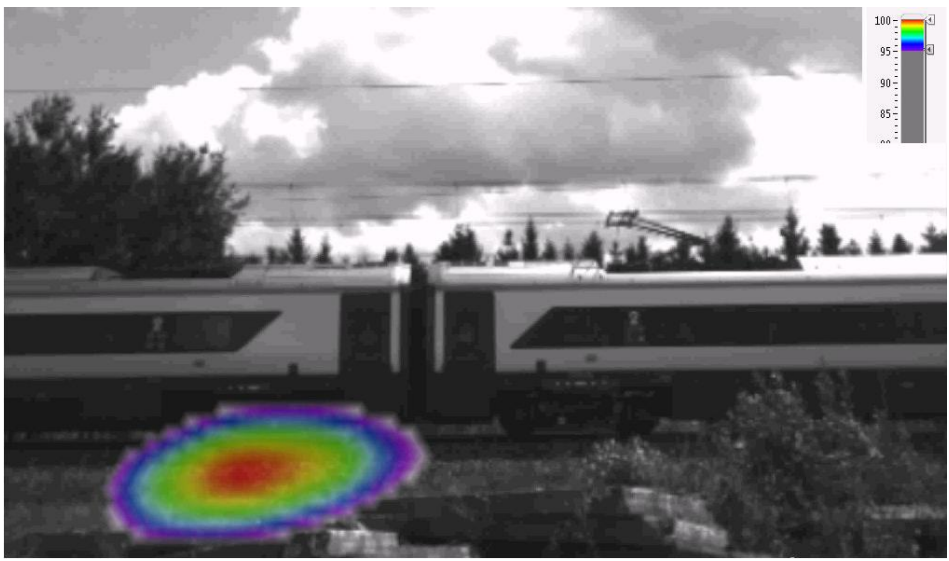

Fig. 4. Sound level distribution in the frequency range 1000-2000 Hz - straight section

On the basis of an experimental study with use of an acoustic camera, the main sources of noise [dBA] from vehicles travelling at 200 km/h on a straight section and on a curve were identified. As a result of the experimental studies, it was indicated that noise resulting from contact phenomena at the wheel-rail interface (rolling noise) and from the operation of the drive units are the dominant sources of sound in the frequency range 500-3000 Hz.

4.2. Identification of dominant frequencies

In the course of the experimental research, 20 high-speed railway vehicle passes were obtained for a straight section and a curve, from which the 10 most authoritative results were then selected, for which 8 signals were obtained, each 20 seconds long, in 31 one-third octave bands from 20 Hz to 20 kHz in two measurement cross-sections (straight section and curve). In addition, the equivalent sound level [dBA] was measured at all points in the measurement cross-section. The data obtained were furtherly analysed in detail.

In order to verify which one-third octave frequencies are characterized by the highest sound pressure levels, the average sound pressure level spectra were determined for the test railway vehicle at the rail head level and at 4 m from the rail head, which travelled along a straight section and a curve. The average sound pressure levels in one-third octave bands at 4 m from railhead level are shown in Table 1.

Table 1. Average sound pressure levels in one-third octave bands at 4m from the rail head level

One-third octave bands [Hz]	5 m		10 m		20 m		40 m	
	Straight section	Curve	Straight section	Curve	Straight section	Curve	Straight section	Curve
20	96,7	96,8	94,1	94,4	90,1	88,8	80,1	79,7
25	97,2	97,1	95,3	95,0	91,0	89,3	81,9	82,2
31,5	97,4	97,3	95,5	95,4	91,1	90,1	84,5	84,6
40	97,7	97,3	96,1	95,4	91,4	91,9	86,0	87,2
50	97,9	97,3	96,2	95,4	91,5	91,6	87,0	89,1
63	97,7	96,9	96,3	94,5	90,0	90,3	87,2	88,8
80	96,8	98,1	94,5	96,8	90,8	91,2	88,3	89,3
100	96,4	97,5	93,8	95,6	88,5	91,2	87,4	89,6
125	95,1	95,9	91,9	92,5	88,0	87,8	83,2	83,7
160	94,7	95,4	91,4	91,6	88,3	85,9	82,0	81,7
200	94,7	95,5	91,4	91,8	86,0	85,1	81,5	81,6
250	94,5	95,7	90,9	92,0	85,7	88,9	81,6	81,8
315	94,4	95,7	90,8	92,1	86,0	88,7	81,2	82,5
400	94,7	95,6	91,2	91,9	87,9	88,4	84,2	82,9
500	95,0	95,7	92,1	92,1	90,2	88,7	85,9	84,2
630	95,5	96,6	92,9	93,8	89,4	90,6	84,8	84,7
800	96,5	98,2	94,9	97,0	91,2	93,3	87,6	87,5
1 000	97,2	100,7	96,3	102,1	93,0	96,7	89,2	91,6
1 250	98,2	100,8	99,6	102,3	94,9	98,1	90,7	92,5
1 600	100,5	101,1	101,4	103,0	99,6	98,9	94,7	94,0
2 000	100,7	100,8	104,0	102,4	101,5	97,6	95,1	93,3
2 500	100,5	99,1	101,3	98,9	98,7	93,8	94,3	89,7
3 150	98,7	97,7	98,6	96,2	96,4	91,6	91,9	87,2
4 000	96,6	95,4	94,8	91,5	89,1	85,3	89,0	80,9
5 000	94,8	94,4	91,6	89,4	84,1	81,7	81,4	76,6
6 300	92,7	92,9	87,7	86,5	81,3	79,9	77,7	74,6
8 000	92,2	91,7	86,6	84,2	79,0	76,8	74,5	70,8
10 000	89,8	89,9	81,5	80,4	75,0	73,8	69,7	67,1
12 500	87,4	88,5	76,8	77,6	68,4	68,8	63,1	61,8
16 000	84,6	86,9	70,8	74,5	59,8	61,2	55,9	55,9
20 000	81,7	85,2	64,9	71,1	56,1	56,8	56,3	56,4

For both situations studied (straight section and a curve), the low bands between 20 Hz and 200 Hz dominate at the level of the rail head in the close vicinity of the railway line (for a distance of 40 m from the track axis), with levels range from 88.3 dB to 96.9 dB. For measurement points located at the height of 4 m from the rail head level (40 m), the highest sound pressure levels are seen in the low bands from 20 Hz to 100 Hz and the medium bands, i.e. from 1000 Hz to 3150 Hz.

Basing on the results, there were shown the dominant frequencies characterizing the passage of high speed vehicles on a curve with a radius of approximately R=4000 m. An analysis of the differences in sound pressure levels (difference of more than 3 dB) for individual one-third octave bands (for the observation point at the height of the rail head) showed that for high speed railway vehicles travelling along a curve, higher values were recorded for bands in the range from 315 Hz to 2000 Hz (difference of 3 to 10.8 dB). In very close proximity to the railway line (5 m), the dominant characteristics also include frequencies: 80 Hz, 100 Hz, 16 000 Hz and 20 000 Hz, for which the maximum differences from the straight section range from 4.3 dB to 5.3 dB.

For the observation point at 4 m above rail head level, individual differences ranging from 3.3 dB to 8.1dB were recorded. The fairly evenly distributed sound pressure levels at 4 m above rail head level indicate that there is an increased proportion of rolling noise on the curve due to the additional friction of the side of the wheel against the rail.

4.3. Sound propagation model

An analysis of the literature shows that there are many methods for the propagation of railway noise. A detailed description of the different models used for the propagation of railway noise has been described in detail in (Komorski et. al. 2022), among others. Models developed in different countries are not suitable for implementation in the operating conditions of other countries, due to differences in rolling stock and track infrastructure structure. This situation confirms the need to develop a suitable noise modelling tool for the high-speed railway vehicle under analysis.

The construction of the sound propagation model started with the verification of the batch data. The data obtained from the 4x2 microphone array was verified by determining the correlation coefficient for all 4 second pairs of representative runs. The standard Matlab high-level language command *corrcoef* was used to determine the correlation coefficients for all pairs of representative runs. The correlation coefficient is defined as the quotient of the covariance and the product of the standard deviations of the tested variables and is determined according to the relationship shown in equation (1) (Metsämuuronen, 2022) or (Sobczyk, 2021):

$$\mathrm{P(A,B)} = \frac{cov\,(A,B)}{\sigma_A \sigma_B} \tag{1}$$

where: *cov(A,B)* - covariance of variables A and B; σ – standard deviation of a given variable.

For the majority of cases, i.e. approx. 99% of cases, the calculated values of the correlation coefficient were not lower than 0.80. The maximum values of the correlation coefficient for the straight section and the curve were equal to 0.998 and 0.999 respectively. In the case of the minimum values of the coefficient, they were equal to 0.431 for the straight section and 0.753 for the curve. After a preliminary analysis of the data obtained, only the crossings with the highest correlation coefficients were selected for further consideration.

The obtained tertiary spectra of sound pressure levels and equivalent sound levels from 10 high speed railway vehicle passages were used to determine statistical parameters, which were the inputs to the propagation models under study. Statistical parameters were defined for each distance from the track axis (i.e., 5 m, 10 m, 20 m, 40 m). The analysis was carried out separately for each height tested, i.e. at the level of the rail head and 4 m above the rail head, separately for each measurement section (straight section and a curve). In order to determine the average level and distribution of values, statistical measures were determined on the basis of representative passages (4 seconds) in the form of a median, which was calculated on the basis of the relationship (Aczel, 2018):

$$Me = \begin{cases} \dfrac{x_{N+1}}{2}; & \text{when N is an odd number} \\ \dfrac{x_{\frac{1}{2}N} + x_{\frac{1}{2}N+1}}{2}; & \text{when N is n even number} \end{cases} \tag{2}$$

Based on the batch data obtained, four selected models for the assessment of railway noise were analysed in terms of their degree of reflection of the

propagation phenomenon. The results of the conducted experimental research were used to verify the behaviour of individual models describing the change of sound level in the i-th frequency band, as a function of variable distance of the observer from the railway line on which high speed railway vehicles are operated. Four models were verified:

– linear (1st degree),
– using a polynomial of 2nd degree,
– using a polynomial of 3rd degree,
– power with free expression.

An example of a noise propagation model fit for all situations investigated is shown in the diagram below (Fig. 5).

On the basis of the noise propagation model fitting analysis, it can be seen that all models behave quite well within the range of measurement points (up to 40 m). The obtained characteristics indicate that the author's model and the power model with free expression in most cases best reproduce the measurement results at specific measurement points as well as at distances up to 60 m from the track axis. The waveforms of the 2nd and 3rd degree models outside the measurement points are characterised by a very large scatter in all ranges of frequency bands and equivalent sound levels. With these results in mind, detailed analyses were limited to the two models that best reflected the propagation phenomenon: the free-expression power model and the author's model.

The next step of the research carried out was to thoroughly verify the representation of the noise propagation phenomenon using a power model with free expression (mp-zww). This model takes the form of (Borwin et al., 2019) or (Szymański et al., 2021):

$$L_i = a_i r^{b_i} + c_i \tag{3}$$

where: L_i – sound pressure level in the i-th frequency band; a_i, b_i, c_i – experimental coefficient of the model for the t-th frequency band; r – distance from the sound source.

The work also included the development and presentation of results for the author's model incorporating band noise correction, which was also subjected to detailed verification in terms of reproducing the propagation phenomenon. The author's model was characterised by good accuracy for the obtained noise propagation levels in terms of the results obtained experimentally at individual measurement points. The analysis of the results obtained for this model, outside the verifiable measurement points, due to the lack of abrupt changes in levels and the linear nature of the decrease in level as a function of further distance, implies a high probability of correctly reproducing the noise propagation phenomenon from increased speed railway vehicles by this model. However, this requires further verification in the form of continuation of future experimental studies.

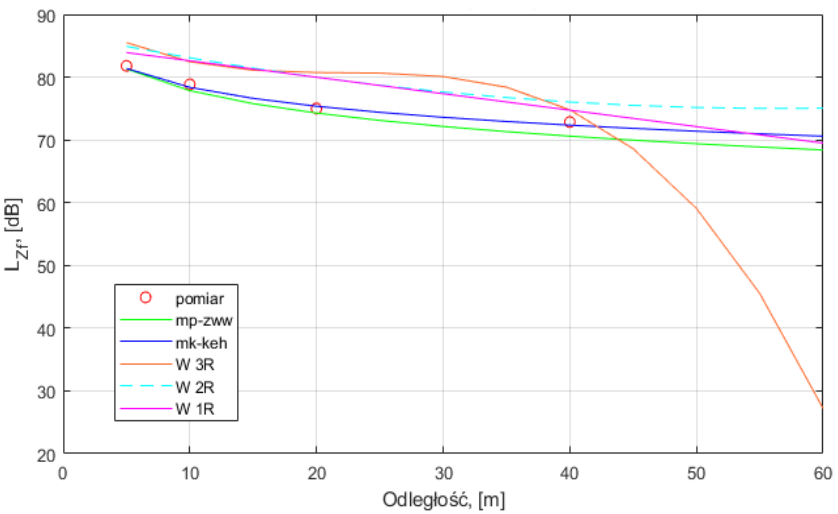

Fig. 5. Fitting of the developed noise propagation model and the free expression potentiometric model for 25 Hz at the rail head level for a straight section

Due to the band analysis of the signal in the relation describing the performance of the model for the i-th frequency band, a level correction kpi was introduced for each of the analysed frequency bands. The relationship describing the level for frequency band i at distance x from the sound source was expressed as:

$$L_{xi} = L_{ri} - 10z\log\frac{x}{r} + k_{pi} \tag{4}$$

Where: L_{xi} – experimentally determined noise level at distance x from the source [dB]; L_{ri} – noise level value measured at reference point r [dB]; z – source type factor (for a linear source z=1); x – distance of observation point from noise source [m]; r – distance of the reference point from the noise source [m]; k_{pi} – level correction for the analysed i-th frequency band [dB].

In order to implement the propagation model scheme for each of the analysed frequencies, an attempt was made to determine the parameters of the models by means of the noise emission correction curve method in Matlab software, through the use of the command - lsqcurvefit (with parameters: describing function, vector of initial conditions, distances of measurement points, sound level values at measurement points). The vector of initial conditions was defined as:

$$x_0 = [s(1)\ s(2)] \tag{5}$$

where: $s(1)$ – noise level at reference point, L_{ri} [dB]; $s(2)$ – correction value for the frequency band, k_{pi} [dB].

The notation of the function took the form:

```
fun = @(s,x_org) (s(1)-
      (10*1*log10(x_org./5))+s(2)),
```
(6)

where x_org was the distance vector of measurement points, hence calling the code *lsqcurvefit* (fun,x0,x_org,y) each time returned the model parameters. Execution of the Matlab function code *nlinfit* (with parameters: distance vector of measurement points, level values at measurement points, function, vector of initial conditions) allowed the model coefficients to be determined. The values of the coefficients for the straight section are shown in Table 2.

The analysis of the author's noise propagation model and the free expression power model showed that both methods have an accurate representation of the results. The model runs show that the free expression power model more accurately reflects the measurement results at specific measurement points, but the differences from the author's model are within error limits. A detailed analysis of the obtained characteristics indicates that the author's model has better waveforms outside the measurement points. The free expression power model, outside the range of measurement points, tends in many cases to reduce noise too quickly as a function of distance, which was also confirmed by detailed analyses in the one-third octave frequency spectra for individual runs. Figures 6-7 show the fitting characteristics of the models used for the wave propagation analyses.

An analysis of the author's noise propagation models showed that the method is characterised by an accurate representation of the results, in most of the frequency ranges investigated. Verification of the obtained characteristics shows that the presented noise propagation model is also characterised by good waveforms outside the measurement points. The absence of abrupt changes in levels and the linear nature of the decrease in level as a function of distance imply a high probability that the noise propagation phenomenon from increased speed railway vehicles is correctly reflected by this model, beyond the measurement points. However, this requires further verification in the form of continued future experimental studies. The obtained results of the author's model were compared with the results from field measurements, which are presented below for example frequencies of the middle one-third octave bands.

4.4. Assessment of acoustic impact on the surroundings

The regulations in Poland stipulate (Ordinance of the Minister of the Environment, 2011) that in built-up areas, measurement points should be located in areas covered by acoustic protection, e.g. at a height of 4 m (+/- 0.2 m) above the ground surface, when it is not possible to take noise measurements in the light of a window on a given floor or in the areas surrounding these buildings. The above solution is the most common way of measuring acoustic signals from linear sources, including railways.

Taking into account the above, only the measurements obtained for a height of 4 m were used for further analysis. As indicated earlier in the previous

part of this article, for a height of 4 m above rail head level, the dominant frequencies ranged from 1 kHz to 3.15 kHz. The results obtained were compared with the MAF-minimum audible field (MAF) threshold (Betke, 1991), which indicates that human hearing sensitivity is highest in the mid-frequency range (1-5 kHz) and decreases markedly in the low- and high-frequency bands (Fig. 8).

Table 2. Coefficient values of the author's noise propagation model

One-third octave bands [Hz]	Straight section				Curve			
	Rail head level		4 m above the rail head level		Rail head level		4 m above the rail head level	
	L_{ri}	k_{pi}	L_{ri}	k_{pi}	L_{ri}	k_{pi}	L_{ri}	k_{pi}
20	93,787	-2,539	93,280	-0,881	98,851	-3,803	97,395	-1,974
25	83,886	-1,302	80,973	-2,334	84,841	-2,461	80,844	-3,078
31,5	84,330	-1,372	81,341	-2,241	85,297	-2,017	81,769	-2,759
40	85,373	-1,833	82,482	-2,143	86,406	-2,056	82,600	-2,532
50	86,555	-1,622	83,016	-2,006	87,362	-2,114	83,273	-2,206
63	87,256	-1,503	83,276	-2,099	86,491	-1,605	83,171	-1,787
80	86,230	-1,306	82,747	-1,995	86,336	-1,891	82,595	-1,896
100	85,367	-1,520	82,383	-1,821	88,337	-2,127	84,816	-2,250
125	83,842	-0,822	80,865	-1,577	87,616	-1,586	83,806	-1,949
160	81,222	-1,256	78,744	-1,538	82,570	-1,617	79,328	-2,056
200	78,642	-0,850	77,625	-1,258	80,316	-1,880	78,030	-2,022
250	76,956	-1,113	76,530	-1,164	78,812	-1,964	77,525	-1,900
315	77,569	-2,319	76,662	-1,483	79,544	-2,795	78,626	-1,656
400	77,320	-3,356	77,054	-1,671	80,489	-4,116	79,730	-2,036
500	76,886	-3,900	77,805	-1,235	80,584	-3,974	79,605	-2,009
630	77,455	-3,988	78,788	-1,146	80,937	-2,981	79,519	-1,637
800	78,176	-3,703	79,415	-1,394	81,848	-2,788	80,984	-1,509
1 000	81,087	-3,202	81,476	-1,173	85,400	-3,769	84,516	-1,930
1 250	79,912	-2,528	81,934	-0,613	88,848	-4,113	88,637	-2,038
1 600	81,170	-2,677	83,766	-0,588	90,226	-4,381	89,767	-2,063
2 000	84,022	-2,291	86,171	-0,287	91,908	-4,077	90,754	-2,065
2 500	85,353	-2,153	88,165	-0,385	90,916	-3,388	89,725	-1,981
3 150	86,717	-2,800	87,037	-0,854	87,875	-3,297	86,126	-2,120
4 000	83,389	-2,522	84,840	-0,648	84,684	-3,177	83,319	-1,909
5 000	79,897	-3,163	80,953	-1,246	79,919	-3,683	78,294	-2,384
6 300	77,242	-3,355	77,234	-2,008	77,389	-4,022	75,641	-2,934
8 000	74,420	-3,992	74,351	-2,188	75,184	-4,247	73,082	-2,924
10 000	73,401	-4,356	73,220	-2,652	72,681	-4,580	70,740	-3,263
12 500	69,884	-4,770	68,740	-2,810	70,353	-4,800	67,536	-3,409
16 000	65,911	-5,444	63,984	-3,596	67,436	-5,738	64,319	-4,116
20 000	61,175	-5,888	57,827	-4,307	64,387	-6,791	60,686	-5,273
$\mathbf{L_{AEq}}$	58,976	-5,511	54,284	-3,867	62,675	-7,013	58,151	-5,016

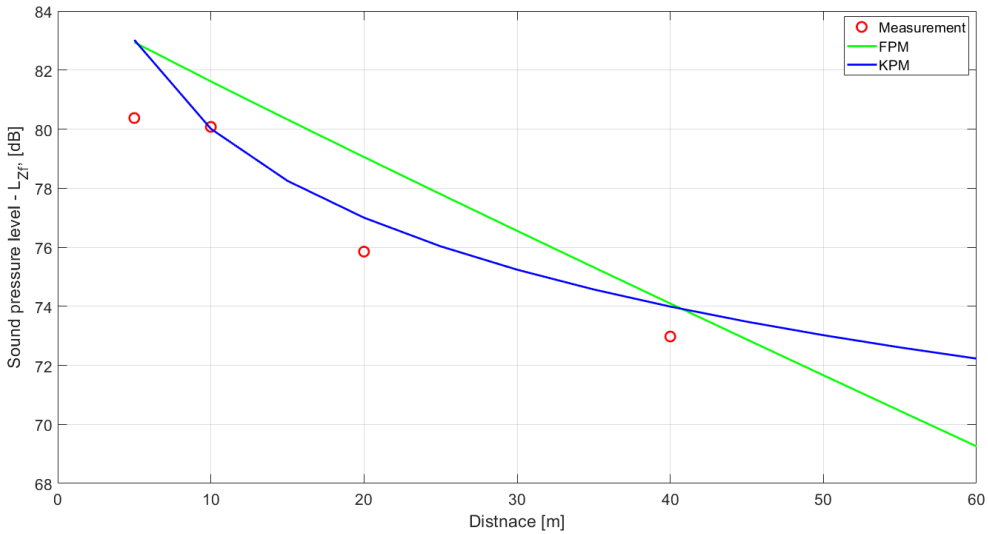

Fig. 6. Fitting of the author's noise propagation model (KPM) and a free expression potentiometric model (FPM) of 100 Hz at rail head level for a straight section

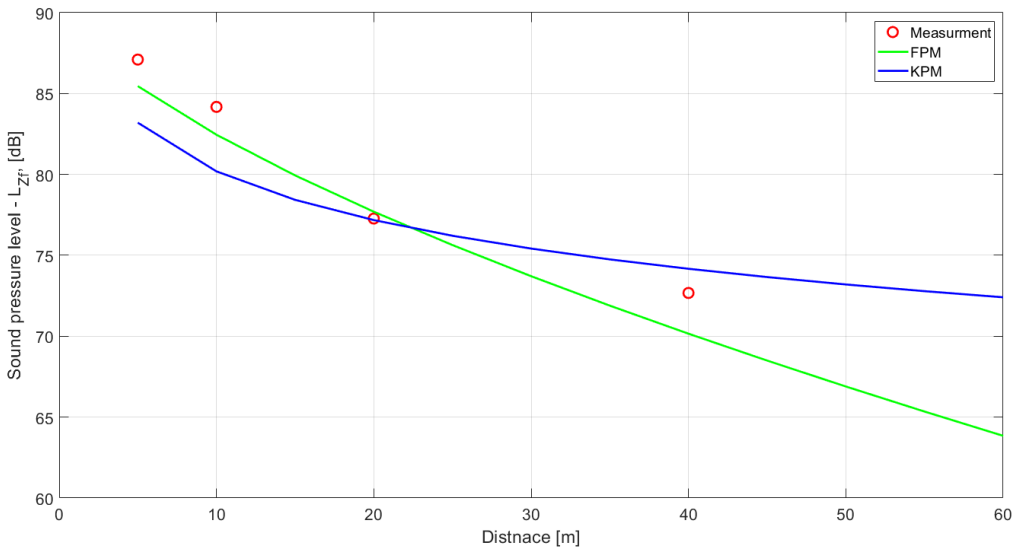

Fig. 7. Fitting of the author's noise propagation model (KPM) and a free expression power model (FPM) for a frequency of 2000 Hz at rail head level for a straight section

It is worth noting that the drop in sensitivity below 1 kHz is about 6dB/octave, while above 5 kHz it is 24dB/octave, due to the resonant nature of the ear canal and the high efficiency of the middle ear functioning in this frequency range (Ozimek, 2018). The analysis showed that the dominant frequencies of the sound pressure levels recorded for a height of 4m from rail head level are within the range of greatest human hearing sensitivity.

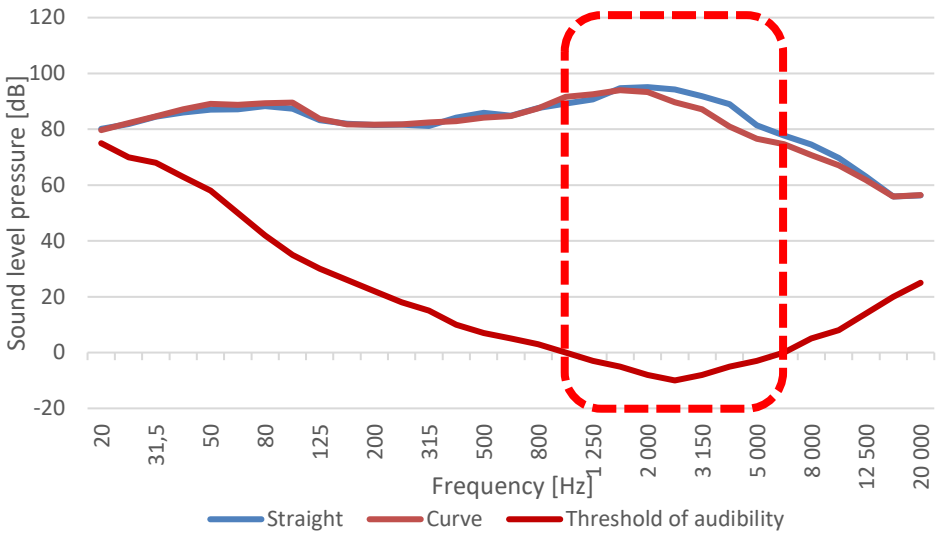

Fig. 8. Comparison of measurement results (straight section and curve for 4 m above rail head level) to human hearing sensitivity (hearing threshold)

5. Summary

In this paper an attempt was made to determine the acoustic signature of a railway vehicle travelling at 200 km/h on a straight section and a curve. As part of the conducted experimental research, test fields were chosen, the measurement apparatus was selected, and the methodology for carrying out measurements including the assessment of noise on a curve and straight section was specified for electric multiple units of Alstom company, type ETR610 - ED250 series, the so-called Pendolino.

Measurements were made using an acoustic camera and a 4x2 microphone array. As a result of the experimental studies, the main sources of noise from the studied object were identified and the dominant amplitude-frequency characteristics in the range from 20 Hz to 20 kHz, divided into one-third octave bands, were identified. In addition, equivalent sound level measurements were made for 20-second passages of high speed railway vehicles, at all points in the measurement cross-section. The experimental studies made it possible to compare the acoustic phenomena recorded separately for a straight section and a curve. The studies confirmed that for electric multiple units travelling at 200 km/h, the dominant noise source is the rolling noise, resulting from vibrations arising at the wheel-rail interface. In the case of high speed rail vehicle passages on a curve with a radius of approx. R=4000m, the noise resulting from wheel-rail vibrations does not unequivocally increase the maximum sound levels compared to a straight section.

The highest sound pressure levels from high speed railway vehicles travelling on a straight section, for heights at the rail head level, were recorded in the low (20 Hz to 160 Hz) and medium (1000 Hz to 4000 Hz) bands. For a height of 4 m above rail head level, the highest levels occurred in the range of 20 Hz to 100 Hz (for a distance of 20 m) and 1000 Hz - 4000 Hz. For vehicles on a curve, the highest values at rail head level were recorded for one-third octave frequencies in the low bands from 20 Hz to 100 Hz (for distances of 40 m) and additionally from 125 Hz to 200 Hz (for 20 m) and in the medium bands from 630 Hz to 3150 Hz (for distances of 20 m). Additionally, for a distance of 40 m, high levels were recorded at 1600 Hz and 2000 Hz. For a height of 4 m above rail head level, high values of sound pressure levels were recorded in the low bands from 20 to 100 Hz (for a distance of 20 m), and for a distance of 40 m in the range of 50 Hz - 100 Hz. High values of sound levels were also recorded for the medium bands in the range from 1000 Hz to 3150 Hz. Basing on the differences in the measured sound pressure

levels, the dominant frequencies in the one-third octave bands (at rail head height), which are characteristic to the passage of high speed railway vehicles on a curve with a radius of R=4000 m, were identified. Differences in sound pressure levels relative to the straight section were recorded for the one-third octave bands between 315 Hz and 2000 Hz.

As part of the work, results were developed and presented for an own model incorporating band noise correction, which was also verified in term of reproducing the propagation phenomenon.

The model had good accuracy for the obtained noise propagation levels in the range of results obtained experimentally at individual measurement points. The analysis of the results obtained for the model (no abrupt changes in levels, linear nature of the decrease in levels) indicates that there is a high probability that the phenomenon of noise propagation from increased speed railway vehicles is correctly reflected by the author's model, also outside the measurement points.

In addition, it has been shown that at a height of 4 m from railhead level, the dominant frequencies are within the range of the greatest hearing sensitivity, i.e. between 1 kHz and 3.15 kHz.

Detailed identification of the acoustic signature of high speed railway vehicles travelling at 200 km/h will enable acoustic impacts to be minimized more effectively. By identifying the main sources of noise and knowing the dominant amplitude-frequency characteristics of the studied object, it will be possible to optimally select solutions and measures to reduce the negative impact of noise on the environment, including, among others, appropriate selection of noise barriers (acoustic screens) aimed at reducing particular frequency bands. In addition, the recognition of amplitude-frequency characteristics can be used, among other things, to diagnose the technical condition of the vehicle and track, which in the long term will make it possible to prevent the occurrence of failures.

References

[1] Abualhayja'a, M., & Hussein, M. (2021). Comparative Study of Adaptive Beamforming Algorithms for Smart antenna Applications. In ICCSPA 2020 - *4th International Conference on Communications, Signal Processing, and their Applications. Institute of Electrical and Electronics Engineers Inc*.. DOI: 10.1109/ICCSPA49915.2021.9385725.

[2] Aczel, A.D., (2018). Statistics in Management, 2nd ed.; PWN: Warszawa, Poland, (In Polish).

[3] Betke K., (1991).New hearing treshhold measurement for pure tones under free-field listening conditions, *J.Acoust. Soc. Am*., 89, 2400-2403.

[4] Borwin M., Komorski , Szymański G., (2019). Modeling of the sound propagation for a railway vehicle moving on the track, *Rail Vehicles* 3/2019, 60-68. DOI: 10.53502/RAIL-138540.

[5] Chiariotti , Martarell M., and Castellini , (2019). Acoustic beamforming for noise source localization—reviews, methodology and applications, *Mech. Syst. Signal Process*, 120, 422–448. DOI: 10.1016/j.ymss2018.09.019.

[6] Czarnecki, M.; Witold, G.; Massel, A.; Walczak, S. (2018). Introduction of High-Speed Rolling Stock into Operation on the Polish Railway Network. In *High-Speed Rail in Poland: Advances and Perspectives*; Zurkowski, A., Ed.; CRC Press: Warsaw, Poland, 203–228. DOI: 10.1201/9781351003308.

[7] Gade S., Ginn B., Gomes J., Hald J., (2015). Recent advances in rail vehicle moving source beamforming, *Sound & Vibration– Instrumentation Reference*, 8-14.

[8] Graf H.R., Czolbe C., (2019). Pass-by noise source identification for railroad cars using array measurements, *Proceedings of the International Congress on Acoustics*, 1574-1581.

[9] Graff M., (2016). The New Electric Multiple Units for Long-Distance and Regional Traffic in Poland in 2015. *Tech. Trans Szyn*, 1-2/2016, 22–33.

[10] He, B.; Xiao, X.-B.; Zhou, Q.; Li, Z.-H.; Jin, X.-S.(2014). Investigation into external noise of a high-speed train at different speeds, *Journal of Zhejiang University: Science A*, 15 (12), 1019-1033. . DOI: 10.1631/jzus.A1400307.

[11] Jiang S., Yang S., Wu D., Wen B-Ch, (2018). Prediction and validation for the aerodynamic noise of high-speed train power car, *Transport Problems*, 13(2), 91-102. DOI: 10.20858/t2018.13.2.9.

[12] Komorski , Szymański G.M., Nowakowski T., (2022). Development of the urban rail vehicle acoustic model, *Applied Acoustics*, 195,

108807, DOI: 10.1016/j.apacoust.2022.108807.

[13] Lan Zhang, Hui Ma,(2021). Investigation of Chinese residents' community response to high-speed railway noise, *Applied Acoustics*, 172, 2021, 107615, DOI: 10.1016/j.apacoust.2020.107615.

[14] Le Courtois F., Thomas J-H., Poisson F., Pascal J-C., (2016). Genetic optimisation of a plane array geometry for beamforming. Application to source localisation in a high speed train, *Journal of Sound and Vibration*, 371, 78-93. DOI: 10.1016/j.js2016.02.004.

[15] Li L., Thompson D., Xie Y., Q. Luo Z.,Lei Z., (2019). Influence of rail fastener stiffness on railway vehicle interior noise, *Applied Acoustics*, 2019, 145, 69-81. DOI: 10.1016/j.apacoust.2018.09.006.

[16] Li M., Zhong S., Deng T., Zhu Z., Sheng X., (2021). Analysis of source contribution to pass-by noise for a moving high-speed train based on microphone array measurement Measurement: J*ournal of the International Measurement Confederation*, 174, 109058. DOI: 10.1016/j.measurement.2021.109058.

[17] Maillard J.,Van-Maercke D., Poisson F., Regairaz J-, Dufour J.B., (2020). Comparison of pass-by railway noise indicators obtained from standard engineering methods with measured values, *Forum Acusticum, Lyon*, 2477-2483. https://dx.doi.org/10.48465/fa.2020.0454.

[18] Meng F, Wefers F, Vorlaender M., (2015). Acquisition of exterior multiple soundsources for train auralization based on beamforming. In: Euronoise 2015, *10theuropean conference on noise control, Maastricht, Netherlands*, 1703.

[19] Metsämuuronen J., (2022) Directional nature of the product–moment correlation coefficient and some consequences *Front. Psychol*. 13:988660. DOI: 10.3389/fpsyg.2022.988660.

[20] Němec, Miroslav, Anna Danihelová, Tomáš Gergeľ, Miloš Gejdoš, Vojtěch Ondrejka, and Zuzana Danihelová, (2020). Measurement and Prediction of Railway Noise Case Study from Slovakia; *International Journal of Environmental Research and Public Health* 17, 10: 3616. DOI: 10.3390/ijerph17103616.

[21] Ozimek, E., (2018). Sound and its perception. In *Physical and Psychoacoustic Aspects*; PWN: Warszawa, Poland. (In Polish).

[22] Polak K, Korzeb J., (2022). Acoustic Signature and Impact of High-Speed Railway Vehicles in the Vicinity of Transport Routes, *Energies*, 15(9), 3244. DOI: 10.3390/en15093244.

[23] Polak K, Korzeb J., (2021) Identification of the major noise energy sources in rail vehicles moving at a speed of 200 km/h, *Energies*, 14(13), 3957. DOI: 10.3390/en14133957.

[24] Polak, K.; Korzeb, J., (2019). Measurements of noise from high-speed rail vehicles, Railway Problems. Pomiary hałasu pochodzącego od pojazdów kolejowych zwiększonych prędkości. *Problemy Kolejnictwa*, 184, 33–38.

[25] Polish Railway Lines Instruction (2009) - Id-12(D29) - List of lines, Introduced by Order No. 1/2009 of the Management Board of PKP Polskie Linie Kolejowe, S.A. of 9 February 2009, as AMENDED., *PKP Polskie Linie Kolejowe* 2009. Available online :https://www.plk-sa.pl/files/ public/user_upload/pdf/Akty_prawne_i_przepisy/Instrukcje/Wydruk/Id-12_Wykaz_linii_06.2021.pdf (accessed on 22 February 2022). (In Polish).

[26] Raczyński, J., (2018). The ED250 (Pendolino) experiences in Poland – first years of exploitation, T*echnika Transportu Szynowego*, no 4/2018, 30-32. Available online: http://yadda.icm.edu.pl/yadda/element/bwmeta1.element.baztech-9b7e36f1-647f-4ee4-aaf5-b0e7d9495dcd/c/Raczynski1TTS4en.pdf (accessed on 27 September 2022).

[27] Ordinance of the Minister of the Environment (2011) of 16 June 2011 on the requirements for carrying out measurements of the levels of substances or energy in the environment by the manager of a road, railway line, tramway line, airport or port. *J. Laws*, 140, 824.

[28] Sheng X., Cheng G., Thompson D.J., (2020). Modelling wheel/rail rolling noise for a high-speed train running along an infinitel long periodic slab track, *J. Acoust. Soc. Am*., 148 (1), 174–190. DOI: 10.1121/10.0001566.

[29] Sobczyk, M., (2021). Statistic; PWN: Warszawa, Poland; EAN: 9788301151997. (In Polish) EAN: 9788301151997.

[30] Szymański, G.M., Misztal, W., Orczyk, M., Komorski , (2021). Modeling of the octave sound spectrum emitted by the F-16 Block 52+ aircraft during takeoff, *Measurement*,

170,108695. DOI: 10.1016/j.measurement.2020.108695.

[31] Uda T., Kitagawa T., Saito S., Wakabayashi Y., (2018). Low frequency aerodynamic noise from high speed trains, *Quarterly Report of RTRI*, 59(2), 109-114. DOI: 10.2219/rtriqr.59.2_109.

[32] Wawrzyniak, A., (2013). Electric team trains of the type ETR610 serie ED250 for PKP Intercity S.A., *TTS Technika Transportu Szynowego*, (9), 20–24.

[33] Zea E., Manzari L.,Squicciarini G., Feng L., Thompson D. Lopez Arteaga I., (2017). Wavenumber–domain separation of rail contributionto pass-by noise, *Journal of Sound and Vibration*, 409, 24–42. DOI: 10.1016/j.js2017.07.040.

[34] Zhang J., Squicciarini G., Thompson D.J., (2019). Implications of the directivity of railway noise sources for their quantification using conventional beamforming, *J. Sound Vib*., 459, 114841. DOI: 10.1016/j.js2019.07.007.

[35] Zhang J., Xiao X., Sheng X., et al., (2019) Sound source localisation for a high-speed train and its transfer path to interior noise., *Chin. J. Mech. Eng.*, 32(59), 1-16. DOI: 10.1186/s10033-019-0375-1.

[36] Zhang J., Xiao X., Wang D.; Yang, Y., Fan, J., (2018)Source contribution analysis for exterior noise of a high-speed train: experiments and simulations, *Shock and Vibration*, 2018, 1-13. DOI: 10.1155/2018/5319460.

[37] Zhao C, Wang P, Yi Q, Sheng X, Lu J., (2018). A detailed experimental study of the validity and applicability of slotted stand-off layer rail dampers in reducing railway vibration and noise, *Journal of Low Frequency Noise, Vibration and Active Control*, 37(4), 896-910. DOI: 10.1177/146134841876596.

[38] Żurkowski A., (2015). Central Trunk Line (CMK) 200km/h. Traffic, timetable and operations, *Technika Transportu Szynowego*, nr 6/2015, 24-25.